Discrimination between Single *Escherichia coli* Cells Using Time-Resolved Confocal Spectroscopy

Joshua B. Edel,[†,‡] Pedro Lahoud,[§] Anthony E. G. Cass,[†] and Andrew J. deMello*[,‡]

Institute of Biomedical Engineering, Department of Chemistry, and Department of Biochemistry, Imperial College London, Exhibition Road, South Kensington, London, SW7 2AZ, United Kingdom

Received: September 25, 2006; In Final Form: October 31, 2006

We describe a technique for rapidly discriminating between single-cell populations within a flowing microfluidic stream. Single-cell time-correlated single-photon counting (scTCSPC) as well as photon burst spectroscopy are used to characterize individual *Escherichia coli* cells expressed with either green, cyano, or yellow fluorescent protein. The approach utilizes standard confocal fluorescence microscopy incorporating femtoliter detection volumes. The measured burst width characteristics are predominately governed by the fluorescence quantum yield and absorption cross section of the proteins used. It is these characteristics which were used to distinguish between cells with high precision. By utilizing scTCSPC individual fluorescence lifetimes originating from single cells could also be determined. Average fluorescence lifetimes are determined using standard deconvolution procedures. The simplicity of the approach for obtaining well-defined burst width distributions is expected to be extremely valuable for single-cell sorting experiments.

Introduction

Significant advances in ultrasensitive detection of fluorescent molecules in liquids at room temperature have been made since the first successful detection of single γ-globulin antibodies (labeled with approximately 100 fluorescein isothiocyanate molecules) in 1976.[1] In the intervening years, developments in high-efficiency photon detectors, high-quality optics, and sample handling techniques have enabled the detection of a wide variety of species at extremely low analytical concentrations. These advances and a recognized need for rapid, on-line measurements at low concentrations have meant that ultrahigh sensitivity detection has found increasing importance and application in biological and chemical analysis.[2−4]

At present, there are a number of distinct approaches applied to the detection of single fluorophores in solution.[5−9] A popular method to achieve single-molecule detection sensitivity adopts the principle of confocal detection.[10−12] In this, a femtoliter probe volume is defined by a focused laser beam (near the diffraction limit) and a confocal pinhole. As a molecule diffuses through this volume it may emit a burst of fluorescence photons (assuming that the molecule possesses a high fluorescence quantum efficiency and low photodegradation rate coefficient), which can be collected and detected. Importantly, the use of femtoliter probe volumes minimizes background signals, which originate from Raleigh and Raman scattering by solvent molecules, due to the reduced number of such molecules in small volumes.

In this publication we develop the concept of confocal spectroscopy to define a simple analysis method that can be used to size and distinguish between cells in freely flowing solution environments. The approach utilizes standard confocal fluorescence microscopy incorporating femtoliter detection volumes. Photon burst and time-correlated single-photon counting (TCSPC) measurements of single cells are used to provide differentiation mechanisms between different cell types. The ability to extract time-resolved (or fluorescence decay time) information when performing detection at the single-molecule level is a relatively new development and allows high-information content measurements to be made on extremely short timescales.[13−17]

The motivation behind the current studies is to improve and simplify existing methods used for single-cell sizing, counting, and recognition. Conventional fluorescence-activated cell sorters are highly efficient; however, they are mechanically complex, require heavy maintenance, and most importantly are costly. The fluorescence-activated cell sorter (FACS) is the most common commercially available cell-sorting technique. To prepare a cell mixture for sorting in a FACS, cells in a suspension are reacted with a fluorescent moiety. Once labeled, the cells are forced to flow rapidly and in single file through the FACS toward a detector, where discrimination is based on a specific optical characteristic (such a color). Up to 30 000 cells/s can be discriminated in modern FACS sorters. Replacing conventional approaches with microfluidic systems can result not only in higher throughput but also reduced costs and sample requirements. Inexpensive devices that rapidly sort live cells, particles, and even single molecules would greatly facilitate screening of combinatorial chemistry libraries or cell populations. Moreover, such devices would have wide applications in clinical medicine and basic biological and materials research.

Recently, there has been interest in integrating cell chemistry with microfluidics.[18,19] Several examples are as follows. Hatch et al. used a microfluidic laminate-based structure incorporating hydrodynamic focusing and flow channels with dimensions less than 1 mm to analyze blood cell samples.[20] Optically transparent

* Corresponding author. E-mail: a.demello@imperial.ac.uk.
[†] Institute of Biomedical Engineering.
[‡] Department of Chemistry.
[§] Department of Biochemistry.

10.1021/jp066267n CCC: $37.00
Published on Web 01/17/2007

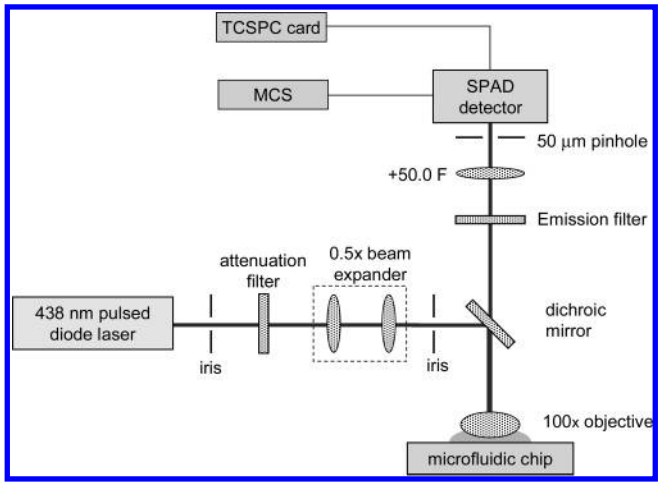

Figure 1. Schematic diagram of the component-based confocal detection optics.

windows integral to the flow channels were used to intercept the sample streams with a tightly focused diode laser probe beam. The size and structure of the blood cells passing through the laser beam determined the intensity and directional distribution of the scattered light generated. Kamholz et al. have also demonstrated the use of microfabricated silicon flow channels and laser light scattering for the differential counting of granulocytes, lymphocytes, monocytes, red blood cells, and platelets, in blood samples.[21] The microfabricated flow cytometer described used hydrodynamic focusing within the microstructure and enlarged optical probe volumes to improve molecular detection efficiencies. More recently, Wheeler et al. have developed a novel microfluidic device for the analysis of single cells that is constructed from polydimethylsiloxane using multilayer soft lithography. The microfluidic network enables the passive and gentle separation of a single cell from the bulk cell suspension. In addition, Fu et al. have designed a disposable microfabricated fluorescence cell sorter (μFACS) for sorting various biological entities.[22] Their μFACS chips resulted in overall higher sensitivity, no cross contamination, and lower overall running costs when compared to those of conventional cell-sorting techniques. The authors were able to successfully separate a diversity of fluorescent particles and also *Escherichia coli* (*E. coli*) cells expressed with green fluorescent protein from nonfluorescing cells. Unfortunately, this approach is limited to the separation of two different types of cells due to the configuration of the confocal spectrometer. The studies described herein extend these ideas by utilizing the photon burst characteristics of single cells as a means of distinguishing between them.

Experimental Section

Confocal Spectrometer. The confocal spectrometer was custom built (Figure 1) and incorporated a 438 nm picosecond pulsed diode laser (PicoQuant GmbH, Berlin, Germany). The diode laser was driven with a PDL 800-B driver also from PicoQuant. The driver unit contains a built in pulse generator which produces a master frequency of 40 MHz that can be divided by factors of 1, 2, 4, 8, and 16 to produce selectable frequencies of 40, 20, 10, 5, and 2.5 MHz. Beam-steering mirrors (BK7 glass, $\lambda/10$ surface flatness, reflectivity >99%; Comar Instruments, Cambridge, U.K.) were used to control the beam height as well as beam direction. A dichroic mirror (470 DRLP02; Omega Optical, Brattleboro, VT) is oriented at 45° to reflect the laser beam radiation and so define a vertical axis, normal to the surface of the optical table. An infinity-corrected, high numerical aperture (NA) microscope objective (Fluar 100×/1.3 NA, oil immersion; Carl Zeiss Ltd., Welwyn Garden City, U.K.) brings the laser light to a tight focus within a microfluidic channel. The laser spot was focused in the center of the fluidic channel (depth and width) removing the possibility of measuring fluorescent signals and lifetimes associated with any surface-bound species. Fluorescence emitted by the sample (within the microfluidic channel) is collected by the same high NA objective and transmitted through the same dichroic mirror. Light is then passed through an emission filter (515EFLP; Omega Optical) to remove any residual excitation light, and a plano−convex lens (+50.2 F; Newport Ltd.) focuses the fluorescence onto a 50 μm pinhole. The pinhole is positioned in the confocal plane of the microscope objective and directly below a silicon avalanche photodiode operating in single-photon counting mode (SPCM-AQR-131; EG&G Canada, Vaudreuil, Quebec, Canada). The detector dark count rate on average is approximately 100 Hz. The precision pinhole is mounted on an *XYZ* translation stage to allow for fine adjustment of the incoming radiation. The electronic signal from the detector is coupled to a multichannel scalar (MCS-PCI; EG&G), running on a Pentium PC as well as to a TimeHarp 200 time-correlated single-photon counting card (PicoQuant GmbH, Berlin, Germany) running on a separate Pentium PC.

***Escherichia coli* Cells.** *Escherichia coli* cells expressed with fluorescent proteins were synthesized according to the following procedure. *Escherichia coli*, strain BL21 Gold (DE3), containing the plasmid encoding fluorescent proteins (living colors range, Clontech, NJ) were grown to midlog phase in LB media (1% tryptone, 1% NaCl, 0.5% Bacto yeast extract) containing 100 μg/mL ampicillin at 37 °C with shaking. Isopropyl β-D-1-thiogalactopyranoside (IPTG) was added to a final concentration of 1 mM, and the temperature was lowered to 30 °C. Cells were allowed to express the protein for approximately 16 h before harvesting by centrifugation at 3220*g* for 10 min at 4 °C. Cells were washed twice in 0.1 culture volumes resuspension buffer (0.14 M NaCl, 1 mM EDTA, 15% glycerol, 10 mM Na_2HPO_4/NaH_2PO_4 pH 7.2) before resuspension to a final concentration of approximately 10^8 cells/mL. Cyano, green, and yellow fluorescent protein were imbedded in all cells. The excitation and emission spectra of these proteins are shown in Figure 2.

Microfluidic Device Fabrication and Operation. Glass microfluidic devices were purchased from Micronit (Enschede, The Netherlands) and comprised a thermally bonded structured glass substrate containing the microchannel network. A simple straight channel microchip design consisting of one input and one output was used for all experiments described herein. The channel widths were 60 μm wide, the channel length was 20 mm, and the channel depth was 30 μm. Coverplates were bonded to etched substrates by heating in a high-temperature oven to a maximum of 610 °C. The top plate was then optically polished down to a thickness of ~150 μm. Optical polishing of the coverplate was performed to reduce the substrate thickness below the working distance of the microscope objective (~150 μm).

Fluorescent cells were hydrodynamically delivered through the microfluidic channel network using a syringe pump (PHD 2000, Harvard Apparatus, Cambridge, MA) at volumetric flow rates between 100 nL/min and 10 μL/min. The detection region was approximately 10 mm downstream of the inlet hole. Both time-resolved and time-integrated measurements involving GFP, CFP, and YFP were performed using the 438 nm pulsed diode laser at a repetition rate of 10 MHz. The laser beam intensity

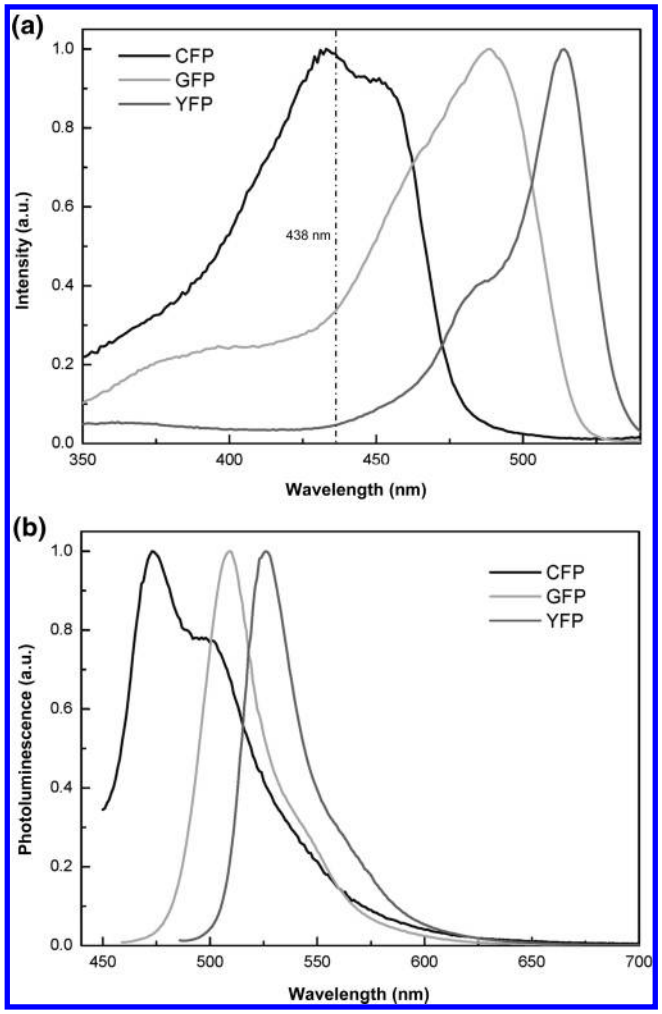

Figure 2. Excitation and emission spectra of cyano, green, and yellow fluorescent protein. The emission maxima are 470, 504, and 525 nm for the cyano, green, and yellow proteins, respectively.

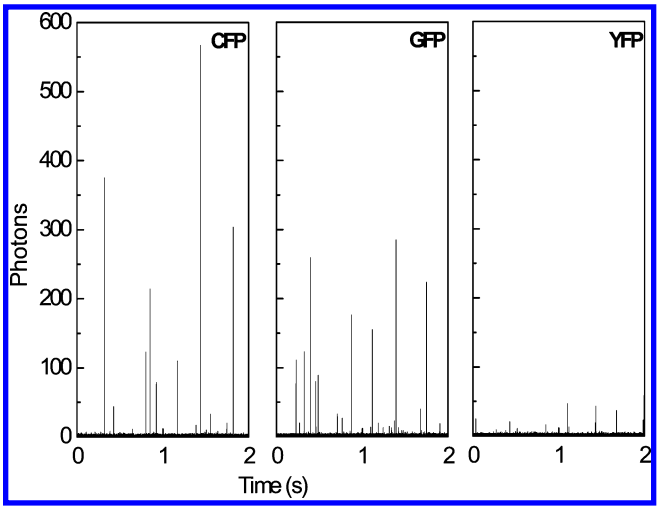

Figure 3. Representative single-cell fluorescence burst scans for *E. coli* expressed with CFP, GFP, and YFP (left−right). The volumetric flow rates in all the plots were 1.0 μL/min.

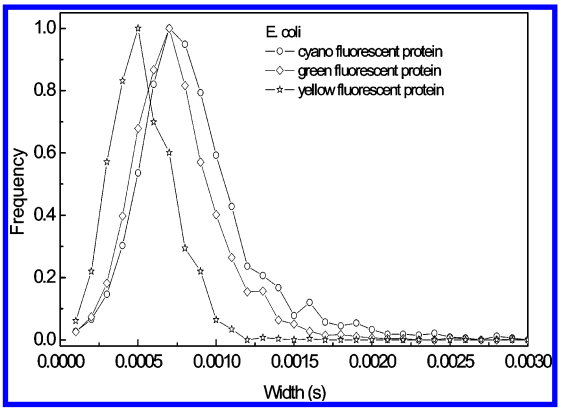

Figure 4. Burst width distributions for *E. coli* expressed with CFP, GFP, and YFP. The flow velocity was 1 μL/min.

was attenuated with a polarization filter as required to obtain an average count rate of 20 000 cps. It was important for a constant excitation wavelength to be used in the analysis of different fluorescent proteins, so as to allow direct comparison of photon burst characteristics in subsequent analysis. The 438 laser line was chosen as both CFP and GFP have an appreciable absorption cross section at that wavelength. This laser line was also used to excite YFP as the onset of absorption occurs at approximately 430 nm (albeit with a much reduced absorption cross section).

Results and Discussion

The volume of an *E. coli* cell can be approximated by a cuboid with dimensions of 1 μm × 1 μm × 2 μm. This results in an internal volume of approximately 2 fL. The final concentration of GFP in solution is approximately 15 μg/mL. This directly results in the concentration of GFP within a cell being approximately 7500 μg/mL. GFP is a protein consisting of 238 amino acids and has an approximate molecular weight of 27 or 30 kDa. Accordingly, it can be deduced that there are a maximum of 500 fluorescent proteins per single cell.

Varying the protein type within the *E. coli* cells results in entirely different burst characteristics (Figure 3). This is attributed to several factors. First, the absorption cross sections of each cell type are markedly different at 438 nm. CFP and GFP have cross sections of ~6×10^3 and ~5×10^3 M^{-1} cm^{-1}, respectively. YFP has an absorption cross section which is approximately 6 times lower than that of GFP. With this in mind, and assuming the cells are expressed with identical protein concentrations, the measured burst heights are expected to be different. A secondary effect on the burst height originates from varying fluorescence quantum yields. The fluorescence quantum yields for CFP, GFP, and YFP are 0.4, 0.6, and 0.7. For the acquisitions shown in Figure 3, the average burst height for CFP was 127 counts with an RSD of 117%. The dwell time in all plots was 100 μs, and the flow rate was constant at 1 μL/min. For GFP-expressed cells under identical conditions, an average burst contained 80 counts and the RSD was 112%. In both cases these values were calculated from 500 bursts over a 65 s period. Burst statistics are significantly worse for YFP. A total of 200 bursts could be detected within a 65 s period at an identical cell concentration. The average burst height was 30 counts; however, the burst height deviation was reduced to an RSD of 85%. This is most likely a result of bursts being hidden in the background noise (which therefore cannot be identified as bursts). The threshold in all three burst scans was 3 ± 0.3 counts; hence the S/N in YFP was typically not larger than 10.

Flow-dependent burst width histograms of the *E. coli* cells exhibit expected trends, i.e., average burst widths and recurrence times decrease with increasing volumetric flow rate. More interesting observations are made in the analysis of burst width histograms. Such histograms are displayed in Figure 4 and are a result of an accumulation of 200 bursts. The flow velocity in all three cases was kept constant at 1 μL/min. The distributions

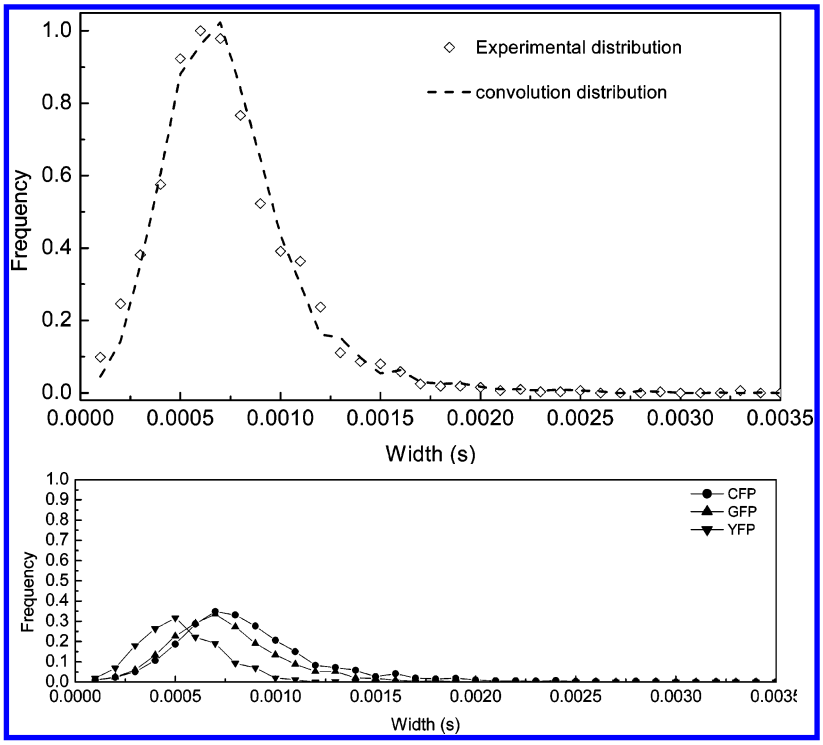

Figure 5. (Top) Burst width histogram for a mixture of 33% of each of CFP, GFP, and YFP (diamonds). The deconvolved distribution is represented by a dashed line. (Bottom) Component distributions for CFP, GFP, and YFP.

are normalized so as to allow for a direct comparison between the different cells. The CFP and GFP histograms are similar in shape due to the absorption cross sections and fluorescence quantum yields being virtually identical in each case. With this in mind the CFP and GFP photon bursts can still be distinguished strictly based on the burst widths. CFP has an average burst width of 922 μs and an RSD of 40%. The GFP cells have a smaller average burst width of 793 μs. In this case the RSD was slightly lower at 33%. Briefly, the burst widths are calculated by searching for a given peak maximum above a specific threshold value which can be defined as 3 standard deviations from the mean count rate, i.e., $n_{\text{threshold}} = \mu + 3(\mu)^{0.5}$. Adoption of a threshold that lies 3 standard deviations above the mean yields confidence limits greater than 99%. The width of the burst above the background level is then measured. The value extracted is in fact a "pseudowidth" as this value is dependent on the signal-to-noise ratio of the peak This is ultimately the cause for different burst widths among the cells expressing different fluorescent proteins.

Escherichia coli expressing YFP exhibit drastically different mean burst width distributions. The average width is 572 μs with an RSD of 31%. The lower burst width is predominantly due to a decrease in the overall photons being collected; this results in an experimental reduction in the burst width. This in fact turns out to be a great advantage as single cells expressing YFP can be distinguished from single cells expressing GFP and CFP strictly based on burst height and width characteristics. Algorithms such as those described by Edel et al. can be useful in assigning single cell types with minimum error.[23] Briefly, they use a maximum likelihood estimator (MLE) to calculate flow velocities of single particles moving through a confocal detection volume. Individual particles with different flow velocities can be distinguished simply based on the analysis of individual fluorescence photon burst characteristics. Although they distinguish between flow velocities, an MLE approach in principle can be used with any system which contains multiple species in solution with different photon burst characteristics. A clear benefit of this approach is that no separation or sorting methods are required to distinguish between cell populations. The majority of microfabricated cell sorters reported in the literature demonstrate sorting with two different cell types. This is primarily due to optical limitations in the instrumentation used. For example, in fluorescence-based cell sorters, there is typically heavy cross talk between detection channels if more than two colors are used, resulting in decreased signal-to-noise and false positives. With the statistical approach described herein, there is no limitation to how many types of cells can be identified. The only requirement is for the fluorophores within the cells to generate different photon burst characteristics.

To develop these concepts further and demonstrate the robustness of the approach a more complex cell population was subsequently studied. Figure 5 illustrates a burst width histogram originating from a mixture of 33% of each of the *E. coli* cell populations (experimental data given by diamonds). In this experiment, the flow velocity was held constant at 1 μL/min with a dwell time of 100 μs. A total of 500 photon bursts were used to generate the histogram. The relative contributions of the burst width distributions for individual components (i.e., the pure samples) were calculated through deconvolution analysis. Specifically, the fitting routine used minimizes the function shown in eq 1.

$$\chi^2 = \sum_{k=1}^{n} \frac{1}{\sigma_k^2}[N(t_k) - N_{\text{CFP}}(t_k) - N_{\text{GFP}}(t_k) - N_{\text{YFP}}(t_k)]^2 \quad (1)$$

Here n is the number of time bins used in the burst width histogram and σ_k is the standard deviation at each data point k. χ^2 denotes the reduced chi squared, $N(t)$ is the least-squares fit, and $N_{\text{CFP}}(t)$, $N_{\text{GFP}}(t)$, $N_{\text{YFP}}(t)$ are the burst width histograms for each of the individual samples. A least-squares fit of the experimental data to this function (shown by the dotted line in Figure 5) produced component yields of 35%, 33%, and 32%, respectively, for CFP, GFP, and YFP. Initial fitting parameters

TABLE 1: Summary of Fluorescence Lifetime Yields and Amplitudes for CFP, GFP, and YFP

	tau 1/ ns	amp 1/ %	tau 2/ ns	amp 2/ %	tau 3/ ns	amp 3/ %	<tau>	χ^2	DW
CFP	3.94	37.80	1.61	34.37	0.22	27.83	3.12	1.12	1.54
GFP	3.21	61.09	1.45	11.11	1.05	27.80	3.04	1.03	1.66
YFP	8.42	2.41	3.23	71.81	0.42	25.78	3.53	1.31	1.41

TABLE 2: Summary of Fluorescence Lifetime Yields and Amplitudes of Bulk Fluorescence Lifetimes for *E. coli* Expressing CFP, GFP, and YFP

	tau 1/ ns	amp 1/ %	tau 2/ ns	amp 2/ %	tau 3/ ns	amp 3/ %	<tau>	χ^2	DW
CFP	7.91	1.41	3.01	58.08	0.96	40.51	2.28	1.13	1.49
GFP	9.44	0.67	2.53	85.92	0.24	13.41	2.69	1.26	1.41
YFP	7.73	4.49	2.70	57.28	0.38	38.23	3.39	1.44	1.20

were randomly generated (and varied at least 10 times) to confirm that the yields produced were not generated by convergence in local minima in the χ^2 hypersurface. In all cases recovered yields did not vary by more than ±1%. It is important to note that the burst width histograms alone cannot be used to discriminate between single cells; rather, they are used to discriminate between populations of cells. Burst intensity and fluorescent lifetimes are ultimately needed for this. The burst width data are simply used for discrimination in an ensemble averaged system.

Decreasing the total number of particles used in the analysis to 100 cells still generated correctly assigned distributions with an error of less than 10%. When experimental distributions were generated using less than 100 cells, the errors associated with the yields were surprisingly not much higher. Nevertheless, this approach successfully extracts valuable information regarding cell populations and can be performed with as little as 100 cells. Lower cell counts can also be used; however, if there are greater than three types of cells within the sample, much larger errors will be associated with the measurement at low precision.

The measurement of fluorescent lifetimes has been used with great success in distinguishing between and quantifying fluorophore populations in complex environments.[24−28] The success of this approach is due to the sensitive dependence of both radiative and nonradiative deactivation rate coefficients on molecular structure and local environment. Consequently, fluorescence lifetime analysis is a sensitive tool for monitoring the nature of samples containing fluorophore populations. The majority of single-molecule lifetime measurements in solution require efficient statistical methods, most notably the MLE, to distinguish between fluorophore lifetimes. However, since the individual cells under investigation in the current studies contain approximately 500 fluorophores, either a MLE algorithm or standard deconvolution procedures can be implemented.

Measurement of the fluorescence decay profiles originating from fluorescent proteins such as CFP, GFP, and YFP using TCSPC techniques has previously shown that simple monoexponential decay functions are insufficient in describing excited-state deactivation. This is a result of complex photophysics involving proton-transfer kinetics. As such, the fluorescence lifetimes are highly dependent on the surrounding environment as well as the excitation wavelength. It is for this reason that the use of bi- or triexponential decay models is typically required to generate physically relevant results. A summary of the component fluorescence lifetimes and amplitudes for CFP, GFP, and YFP in bulk solution is presented in Table 1. The excitation source was a 438 nm pulsed diode laser with emission being collected between 450 and 650 nm. Furthermore, all decays were

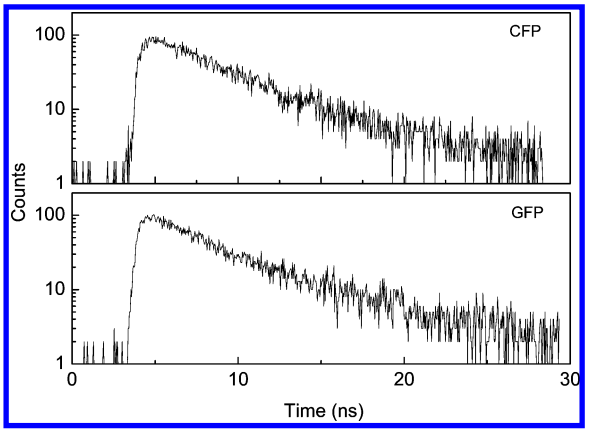

Figure 6. Average fluorescence lifetime decays for single *E. coli* cells expressing CFP and GFP.

measured to yield between 20 000 and 30 000 counts in the channel of maximum intensity.

The lifetime analysis for *E. coli* cells expressed with fluorescent proteins, under the same conditions as described in the previous paragraph, generated drastically different component lifetimes. In all three cases the longest components had lifetimes on the order of 8−10 ns and amplitudes varying from 1−5%. The lifetimes and associated pre-exponential factors obtained for *E. coli* expressing green fluorescent protein are similar to those reported by Jakobs et al. using a similar instrumental setup.[29] A complete summary of the amplitudes along with the lifetimes is shown in Table 2.

The average lifetimes for *E. coli* expressing CFP, GFP, and YFP were 2.28, 2.69, and 3.39 ns respectively. For all three proteins, the component which produced the largest amplitudes (>57%) had lifetimes ranging from 2.5−3 ns. Although the bulk lifetimes are in themselves relatively complex in nature, the variation in average lifetime between the cell populations is sufficiently large to allow cell-type identification at a single-cell level. It should be emphasized that each cell contains a minimum of 500 protein molecules; hence, the lifetimes can still be considered to be an ensemble measurement.

The fluorescence lifetime for two different single cells expressed with CFP and GFP are shown in Figure 6. For these measurements a volumetric flow rate of 1 μL/min and an acquisition dwell time of 100 μs were used. Under such conditions, individual cells remain within the detection probe volume for less than 1 ms; hence, precision when compared to the ensemble (bulk) fluorescence measurements will be significantly poorer. On average, a single-cell decay profile is the accumulation of between approximately 1000 and 5000 photons (~100 counts in the channel of maximum intensity). The error associated with the measurement will therefore be on the order of 10%. When compared to the bulk lifetimes, an accumulation of between 10^5 and 10^6 photons are typically acquired.

Fluorescence lifetime histograms for single *E. coli* cells expressed with CFP and GFP are shown in Figure 7. In all experiments the average residence time of a cell within the probe volume is approximately 100 ms. As previously discussed, due to the low levels of precision data were analyzed using a monoexponential decay function. The average lifetimes from the histograms are calculated to be 2.3 and 2.7 ns for CFP and GFP, respectively. The standard deviation in the single-cell histograms for CPF and GFP were 0.4 and 0.2 ns, respectively. Both average values agree well with the average fluorescence lifetime elucidated in bulk solution experiments. It is reassuring

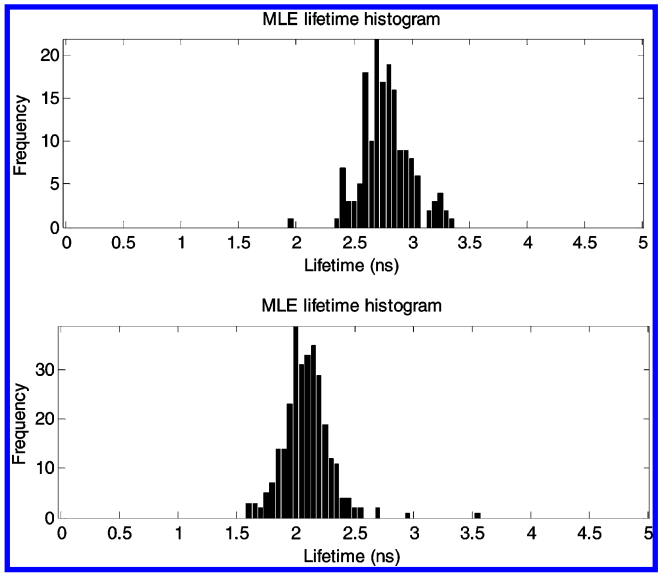

Figure 7. Lifetime histogram from an accumulation of single *E. coli* cells expressed with GFP (top) and CFP (bottom).

to note that even with such similar fluorescence lifetimes between the two types of cells, it is still possible to discriminate between single cells passing through the optical probe volume. On the basis of these observations, the measurement of single-cell lifetimes along with respective burst heights and widths appears to be a powerful approach to discriminating and counting different cell types. It should be noted that for the current experiments, fluorescence lifetime histograms for single *E. coli* cells expressed with YFP were not performed as the total number of bursts registered was not sufficient to obtain statistically reliable information pertaining to the distribution.

Conclusions

A high-sensitivity technique has been developed to discriminate between different cell populations within flowing fluidic streams. The approaches described can be used in single-cell sizing and counting applications with high precision. The method uses the measurement of single-cell fluorescence lifetimes, as well as burst width histograms, to characterize individual fluorescent cells traveling through a femtoliter probe volume. The simplicity of the approach for obtaining well-defined burst width distributions should be extremely valuable for single-cell sorting experiments. In the approach taken herein, we are able to use a subfemtoliter probe volume while controlling the shape of the burst width histogram without making any changes to the basic confocal microscopic experiment. Strictly using photon burst characteristics, it is possible to discriminate between various analyte populations. Single-cell fluorescence lifetime measurements are shown to be a powerful tool in discriminating between *E. coli* cells expressed with various fluorescent proteins. Larger differences between fluorescence lifetimes directly results in greater precision in classification of cell types. Nevertheless, fluorophores with relatively small differences in lifetime can still be discriminated by acquiring a larger number of events.

References and Notes

(1) Hirschfeld, T. *Appl. Opt.* **1976**, *15*, 2965.
(2) deMello, A. J. *Nature* **2006**, *442*, 394.
(3) Craighead, H. *Nature* **2006**, *442*, 387.
(4) Dittrich, P. S.; Manz, A. *Anal. Bioanal. Chem.* **2005**, *382*, 1771.
(5) Dittrich, P. S.; Schwille, P. *Anal. Chem.* **2002**, *74*, 4472.
(6) Zhang, P.; Tan, W. *Chem.—Eur. J.* **2000**, *6*, 1087.
(7) van Orden, A.; Keller, R. A.; Ambrose, W. P. *Anal. Chem.* **2000**, *72*, 37.
(8) Prummer, M.; Hübner, C. G.; Sick, B.; Hecht, B.; Renn, A.; Wild, U. P. *Anal. Chem.* **2000**, *72*, 443.
(9) Ma, Y.; Shortreed, M. R.; Yeung, E. S. *Anal. Chem.* **2000**, *72*, 4640.
(10) Stavis, S. M.; Edel, J. B.; Samiee, K. T.; Craighead, H. G. *Lab Chip* **2005**, *5*, 337.
(11) Stavis, S. M.; Edel, J. B.; Li, Y. G.; Samiee, K. T.; Luo, D.; Craighead, H. G. *Nanotechnology* **2005**, *16*, S314.
(12) Royer, C. A. *Chem. Rev.* **2006**, *106*, 1769.
(13) Enderlein, J.; Ambrose, W. P. *Appl. Opt.* **1997**, *36*, 5298.
(14) Kollner, M.; Wolfrum, J. *Chem. Phys. Lett.* **1992**, *200*, 199.
(15) Sauer, M.; Angerer, B.; Han, K. T.; Zander, C. *Phys. Chem. Chem. Phys.* **1999**, *1*, 2471.
(16) Sauer, M.; Arden-Jacob, J.; Drexhage, K. H.; Gobel, F.; Lieberwirth, U.; Muhlegger, K.; Muller, R.; Wolfrum, J.; Zander, C. *Bioimaging* **1998**, *6*, 14.
(17) Zander, C.; Drexhage, K. H.; Han, K. T.; Wolfrum, J.; Sauer, M. *Chem. Phys. Lett.* **1998**, *286*, 457.
(18) El-Ali, J.; Gaudet, S.; Gunther, A.; Sorger, P. K.; Jensen, K. F. *Anal. Chem.* **2005**, *77*, 3629.
(19) El-Ali, J.; Sorger, P. K.; Jensen, K. F. *Nature* **2006**, *442*, 403.
(20) Hatch, A.; Kamholz, A. E.; Hawkins, K. R.; Munson, M. S.; Schilling, E. A.; Weigl, B. H.; Yager, P. *Nat. Biotechnol.* **2001**, *19*, 461.
(21) Kamholz, A. E.; Weigl, B. H.; Finlayson, B. A.; Yager, P. *Anal. Chem.* **1999**, *71*, 5340.
(22) Fu, A. Y.; Spence, C.; Scherer, A.; Arnold, F. H.; Quake, S. R. *Nat. Biotechnol.* **1999**, *17*, 1109.
(23) Edel, J. B.; deMello, A. J. *Phys. Chem. Chem. Phys.* **2003**, *5*, 3973.
(24) Lakowicz, J. R. *Principles of Fluorescence Spectroscopy*; Plenum Press: New York, 1983.
(25) Maus, M.; Cotlet, M.; Hofkens, J.; Gensch, T.; De Schryver, F. C.; Schaffer, J.; Seidel, C. A. M. *Anal. Chem.* **2001**, *73*, 2078.
(26) Enderlein, J. *Chem. Phys. Lett.* **1999**, *301*, 430.
(27) Kollner, M.; Fischer, A.; ArdenJacob, J.; Drexhage, K. H.; Muller, R.; Seeger, S.; Wolfrum, J. *Chem. Phys. Lett.* **1996**, *250*, 355.
(28) Tellinghuisen, J.; Goodwin, P. M.; Ambrose, W. P.; Martin, J. C.; Keller, R. A. *Anal. Chem.* **1994**, *66*, 64.
(29) Jakobs, S.; Subramaniam, V.; Schonle, A.; Jovin, T. M.; Hell, S. W. *FEBS Lett.* **2000**, *479*, 131.